



# Performance evaluation of discrete Raman amplifiers in coherent transmission systems

PRATIM HAZARIKA,<sup>1,\*</sup>  MINGMING TAN,<sup>1</sup>  MD ASIF IQBAL,<sup>2</sup>   
IAN PHILLIPS,<sup>1</sup>  PAUL HARPER,<sup>1</sup> JEFFERY S. STONE,<sup>3</sup>  
MING JUN LI,<sup>3</sup>  AND WLADEK FORYSIAK<sup>1</sup> 

<sup>1</sup>Aston Institute of Photonic Technologies, Aston University, Birmingham B4 7ET, United Kingdom

<sup>2</sup>BT Applied Research, Adastral Park, Ipswich IP5 3RE, United Kingdom

<sup>3</sup>Corning Incorporated, 1 Riverfront Plaza, Corning, NY 14831, USA

\*p.hazarika@aston.ac.uk

**Abstract:** We evaluate the performance penalty due to discrete Raman amplifier (DRA) in a long haul WDM transmission system. The investigation was primarily performed to study the impact of the accumulated nonlinear noise due to fibre chromatic dispersion and nonlinear coefficient ( $\gamma$ ). Nonlinear fibres such as inverse dispersion fibre (IDF), dispersion compensation fibre (DCF) and a development fibre known as the Corning Raman fibre (CRF) with the opposite sign of CD to the other two, were taken as the gain fibre in the DRA stage of the long-haul transmission setup. To study the performance penalty with these Raman gain fibres a 30 GBaud 120 Gb/s DP-QPSK channel @1550 nm was combined with 9 spectrally shaped 50 GHz amplified spontaneous emission (ASE) channels for transmission over a recirculation loop with a per loop length of 63 km single mode fibre (SMF). Our modelling and experimental results show that a fibre with positive dispersion  $>10\text{ps/nm/km}$  and a nonlinear coefficient of  $\sim 4\text{W}^{-1}\text{km}^{-1}$  is a good choice of gain fibre for DRA-assisted coherent transmission system.

Published by Optica Publishing Group under the terms of the [Creative Commons Attribution 4.0 License](https://creativecommons.org/licenses/by/4.0/). Further distribution of this work must maintain attribution to the author(s) and the published article's title, journal citation, and DOI.

## 1. Introduction

Transmission systems based on C + L-band erbium-doped fibre amplifiers (EDFAs) can support  $\sim 100\text{ nm}$  of the optical window with a parallel approach of amplification for each band [1]. However, extending the bandwidth beyond this spectral range is not possible with existing EDFA based amplification technology. Discrete Raman amplifiers (DRAs), on the other hand, are an alternative solution which can support seamless amplification across a wide spectral range [2–4], enabling multi band transmission (MBT) over the low loss window of single-mode fibre (SMF) [5,6]. The spectral bandwidth of the DRA is completely flexible, and can provide arbitrary gain [7] across a bandwidth greater than  $100\text{ nm}$  [8], using multiple pumps with low relative intensity noise (RIN) [9] selected at suitable wavelengths and powers. Experimental demonstration has already shown an amplification bandwidth of  $150\text{ nm}$  comprising the S, C and L bands, with a net gain of  $15\text{ dB}$  and a maximum noise figure (NF) of  $\sim 8\text{ dB}$ , using a dual stage DRA [10]. In terms of maximum achievable gain, a record gain of  $27\text{ dB}$  with an average NF of  $5.8\text{ dB}$  with a dual stage DRA has been reported in [11]. The length of the Raman gain fibre is usually in the  $\text{km}$ 's range for a DRA-assisted transmission system, and therefore the accumulated nonlinear noise in each amplifier section can add up significantly with increase in the transmission distance consequently degrading the transmission performance. A preferable fibre for use in DRAs is one with a high value of Raman gain coefficient ( $g_r$ ) [12]. However, the DRA fibre chromatic dispersion (CD) and nonlinear coefficient ( $\gamma$ ) can also significantly affect the generation and accumulation of nonlinear noise.

Our previously reported work on the performance penalty due to CD was performed using a single 23 GBaud QPSK channel in a long-haul transmission system [13] with DCF and CRF as the gain fibres. In single channel transmission the nonlinear noise accumulation is only due to the self-phase modulation (SPM) component, without the effect of cross phase mixing (XPM) and four wave mixing (FWM) due to the absence of any neighboring channels. However, in a real time WDM system, the performance of a given channel under test (CUT) degrades due to the combined effect of SPM, XPM and FWM components arising due to pulse propagation in the nonlinear media [14,15]. In this paper, we extend this work to multichannel long-haul transmission system to analyze the performance penalty of different fibre types with varying value of CD and nonlinear coefficient ( $\gamma$ ). For our test cases, we considered inverse dispersion fibre (IDF), dispersion compensation fibre (DCF) and a new development fibre, here named Corning Raman fibre (CRF) [13,16] as the candidate gain fibres for usage in the DRA stage of a WDM transmission link. To analyze the trend in the performance penalty due to the variation in fibre CD and nonlinear coefficient ( $\gamma$ ) the analytical model presented in [17] was used to calculate the accumulated nonlinear noise taking into consideration a hypothetical DCF-like fibre in the gain stage of the DRA. Our modelling results show that fibre with a positive value of dispersion and a nonlinear coefficient of  $\sim 4 \text{ W}^{-1}\text{km}^{-1}$  similar to IDF would be a good choice for a gain fibre in DRA-assisted transmission systems. To experimentally study the performance of DRAs with positive and negative values of CD, a long-haul transmission was performed using a recirculation loop with DCF, CRF and IDF as the gain fibre in the DRA stage of the transmission link. A 30GBaud DP-QPSK signal was combined with 9 spectrally shaped 50 GHz amplified spontaneous emission (ASE) channels over a long-haul recirculation loop. Only 10 WDM channels were taken for our experimental demonstration as the nonlinear noise accumulation is primarily due to the presence of the neighboring channels to the CUT. Our experimental results show an improved performance of positive dispersion CRF over negative dispersion DCF indicating the performance benefits of positive CD over negative CD when the remaining parameters of the fibres are considerably similar. However, slight improvement in the performance of IDF over CRF was observed due to the low linear noise figure (NF) and nonlinear coefficient ( $\gamma$ ) of IDF over CRF.

## 2. Analytical model

A simplified signal power distribution in a typical optical link Fig. 1 a) (transmission fibre followed by a discrete Raman amplifier) is shown in Fig. 1 b).

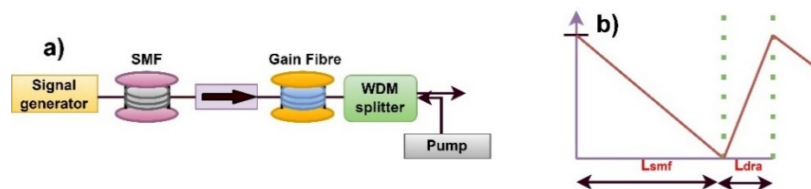


**Fig. 1.** a) Schematic of a single span transmission with backward pumped discrete Raman amplifier b) Amplified links with log signal power profile.

The SMF span loss is compensated by the gain of the DRA. The accumulated nonlinear product power ( $P_{NL}$ ) in such a fibre link can be represented by an analytical representation of the piece-wise signal profile approximation (SMF loss section + DRA gain section), an extension of the theoretical model presented in [17,18]. The spectral location of this nonlinear product at frequency,  $\omega_F$ , depends on the three interacting optical waves at frequencies  $\omega_i$ ,  $\omega_j$  and  $\omega_k$  such

that  $\omega_F = \omega_i + \omega_j - \omega_k$  [19–21].

$$P_{NL} = \left(\frac{D}{3}\right)^2 P_i P_j P_k^* \left[ \frac{\sin^2(N\beta L)}{\sin^2(\beta L)} \right] \left| \gamma_{smf} \frac{e^{(-\alpha+i\beta_{smf})L_{smf}} - 1}{-\alpha+i\beta_{smf}} + \gamma_{dra} e^{\left[(-\alpha+i\beta_{smf})\frac{L_{smf}}{2}\right]} \frac{e^{(g_{dra}+i\beta_{dra})L_{dra}} - 1}{g_{dra}+i\beta_{dra}} \right|^2 \quad (1)$$

$$\beta_{smf/dra} = \frac{2\pi\lambda_{coi}^2}{c} (\omega_i - \omega_k)(\omega_i - \omega_j) CD_{smf/dra} \quad (2)$$

Here,  $P_{NL}$  is the accumulated nonlinear power,  $D$  is the degeneracy factor ( $D = 1$ , when  $\omega_i = \omega_j = \omega_k$  for self-phase modulation (SPM),  $D = 3$ , when  $\omega_i = \omega_j \neq \omega_k$ . for cross-phase modulation (XPM) and  $D = 6$ , when  $\omega_i \neq \omega_j \neq \omega_k$  for four wave mixing (FWM)),  $P_i$ ,  $P_j$ , and  $P_k$  are the powers of the three interacting waves launched into the span,  $N$  is the number of periodic unit cell (SMF + DRA) spans,  $\beta_{smf/dra}$  is the phase matching coefficient for the SMF or the DRA fibre section represented by Eq. (2), where  $\lambda_{coi}$  is the wavelength of the channel of interest which is 1550 nm in our case,  $c$  is the speed of light,  $\omega_i$ ,  $\omega_j$  and  $\omega_k$  are the frequencies of the three nonlinear components and  $CD_{smf/dra}$  is the fibre CD for the SMF or the DRA section [22].  $L = L_{smf} + L_{dra}$  is the sum of SMF fibre span length and the DRA fibre length,  $\beta L = \beta_{smf}L_{smf} + \beta_{dra}L_{dra}$  is the effective phase matching coefficient for each periodic unit cell,  $\alpha$  is the attenuation coefficient,  $g_{dra}$  is the Raman gain coefficient,  $\gamma_{smf}$  is the nonlinear coefficient for SMF and  $\gamma_{dra}$  is the nonlinear coefficient of the corresponding DRA fibre. The system performance may be estimated from

$$SNR = \frac{P_s}{P_{ASE} + P_{NL}}. \quad (3)$$

The ratio of the signal power spectral density,  $P_s$ , to the total noise spectral density comprising the linear ASE noise ( $P_{ASE}$ ) and the accumulated nonlinear noise ( $P_{NL}$ ). The parameters of the different fibre types used in the analytical model are given in Table 1, where the Raman amplifier noise figures were obtained from experimental measurements over the given fibre lengths, for fixed input powers of -8 dBm, and 1455nm Raman pump powers were adjusted to give ~13dB gain in each case (SMF measurements not required).

**Table 1. Summary of fibre and amplifier parameters @1550 nm used in the analytical modelling**

Fibre type	Attenuation coefficient (dB/km)	Chromatic dispersion (ps/nm/km)	Nonlinear coefficient ( $W^{-1}km^{-1}$ )	Peak Raman gain coefficient ( $W^{-1}km^{-1}$ )	Noise Figure (dB)	Effective area ( $\mu m^2$ ).	Fibre length (km)
IDF	0.23	-44	3.53	1.3	6.1	31	10.1
DCF	0.51	-96	8.43	1.8	6.6	19	8
CRF	0.44	11.7	8.87	1.95	6.6	17	8.25
SMF	0.2	16.5	1.3	0.43	X	80	63

### 3. Raman amplifier parametric analysis with the analytical model

The performance of a DRA-assisted coherent WDM transmission system depends on multiple parameters of the transmission and gain fibre [23]. The length of a gain fibre for any target net gain varies significantly with the different fibre type. Fibres such as highly nonlinear fibre with typical peak Raman gain coefficient ( $g_r$ ) of  $\sim 6.9 W^{-1}km^{-1}$  [11] require lower length for achieving a target gain. Similarly, to achieve the same net gain with fibres such as IDF, requires longer fibre and increased pump power.

An important parameter that can also impair the transmission performance of a fibre link is fibre CD. The accumulation of CD causing pulse broadening is compensated using digital

signal processing (DSP) in the receiver stage for signal recovery. However, CD in the gain fibre of the DRA stages also varies the nonlinear accumulated noise for a given channel of interest (COI). The phase matching coefficient  $\beta$  depends on the sign and value of the fibre CD (Eq. (3)) [24,25] hence, for a fibre link with multiple DRAs, the sign and value of CD in the gain fibre can strongly impact the overall system performance. To study the effect of residual dispersion we considered a hypothetical DCF-like fibre in the DRA stage of our model in a set of single channel simulations, evaluating the SNR using Eq. (1-3), at a channel wavelength of 1550 nm (50 GHz bandwidth). The CD parameter of this hypothetical test fibre was varied from -100 ps/nm/km to 40 ps/nm/km keeping the remaining fibre parameters fixed. A SNR variation of  $\sim 2.1$  dB was observed between the highest positive and least negative values of fibre CD from these modelling results, as shown in Fig. 2(a). This test case also somewhat resembles a comparison of DCF and CRF, whose parameters are approximately similar, except for the value of CD, as shown in Table 1. The modelling results for this particular test case show that a Raman gain fibre with positive CD is a better choice for a DRA transmission system.

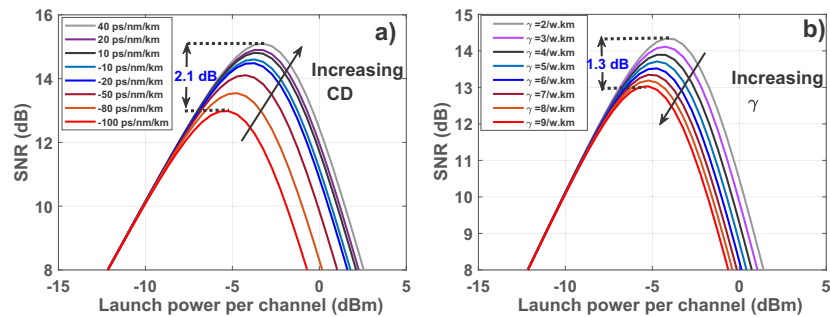


**Fig. 2.** SNR vs launch power per channel to SMF (single channel @ 1550 nm) for  $30 \times 63$  km transmission link with varying values of a) chromatic dispersion b) nonlinear coefficient ( $\gamma$ ).

The nonlinear accumulated noise also depends on the nonlinear coefficient ( $\gamma_{dra}$ ) of the DRA gain fibre. To analyze the performance penalty in a fibre link with varying  $\gamma_{dra}$  we calculated the corresponding SNR with varying launch power in a  $30 \times 63$  km SMF link with another hypothetical DCF-like DRA gain fibre. All the parameters of the hypothetical DCF were fixed except for the nonlinear coefficient which varied from 2 to 9  $W^{-1}km^{-1}$ . The modelling results in Fig. 2(b) shows a maximum SNR variation of  $\sim 1.3$  dB over the entire range of nonlinear coefficient. However, an important point to note here is that a lower value of  $\gamma$  might also result in insufficient gain due to the lower value of Raman gain coefficient ( $g_{dra}$ ), and the power limitations of commercially available pumps. Overall, the results of Fig. 2(a) and (b) suggest that a DRA fibre with positive dispersion ( $> 10$  ps/nm/km) and a moderate nonlinear coefficient ( $\sim 4$   $W^{-1}km^{-1}$ ) would be a good choice for DRA-assisted coherent transmission system.

#### 4. Experimental setup

To evaluate the dependence of fibre CD and nonlinear coefficient experimentally we conducted a long haul WDM transmission experiment with a recirculation loop as illustrated in Fig. 3. Nine spectrally shaped ASE signals of 50 GHz bandwidth were combined with a 120Gb/s 30 GBaud polarization multiplexed DP-QPSK signal at 1550 nm generated using a commercial transponder, to form a 10 channel WDM grid (1546.05 nm to 1553.3 nm). The WDM channels were then passed through a transmitter (Tx) EDFA and a variable optical attenuator (VOA) for launch power sweep. The recirculation loop comprised of two acousto-optic modulators (AOMs) and a 3 dB coupler followed by a 63 km length of SMF. The 3 dB coupler was followed by an optical isolator to prevent any signal back-reflection and a 99/1 tap was added to the bre input section to

monitor the launch power to the fibre. The DRA stage comprised either a DCF, CRF or IDF with span lengths of 8 km, 8.25 km and 10.1 km respectively, pumped with a 1455 nm laser source in backward configuration, to compensate for the combined SMF and WDM coupler loss of 12.4 dB. The required pump powers were 448 mW, 380 mW and 582 mW for DCF, CRF and IDF respectively. A dynamic wavershaper (WSS) was included in the loop section to flatten the optical spectrum after each recirculation. An additional  $\sim 18$  dB loop loss (comprising 6.5 dB, 4dB and 3.5dB due to the WSS, AOMs and 50/50 coupler, respectively, 1 dB due to the isolator and 99/1 tap, and the remaining 3 dB due to WSS levelling and multiple FC/PC and FC/APC connectors combining these components) was compensated using an EDFA with a NF of  $\sim 6$  dB.

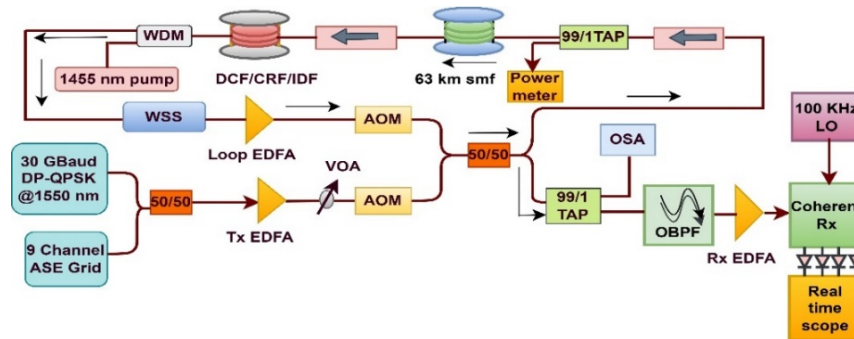


**Fig. 3.** Recirculation loop experimental setup for WDM transmission.

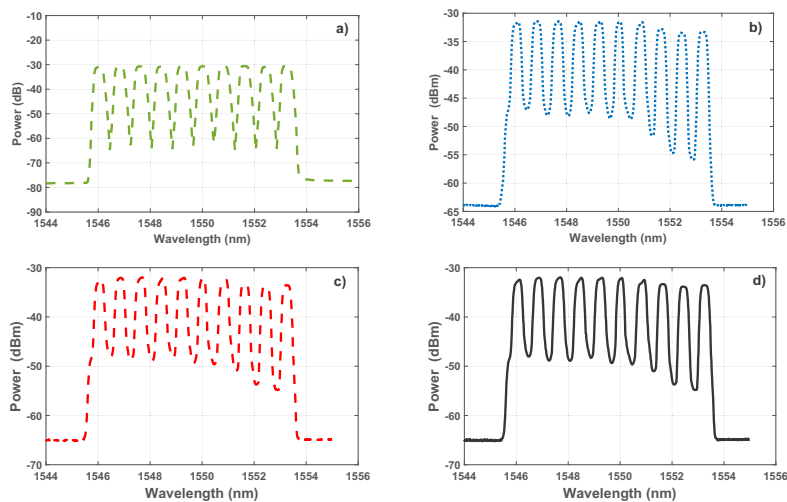


**Fig. 4.** Optical spectrum of 10 WDM channels a) input spectrum; 20 span transmission with DRA stage comprising of b) DCF c) CRF d) IDF.

The receiver (Rx) section included a 99/1 tap whose 1% arm was used to monitor the output spectrum, while the remaining 99% was passed through a tuneable optical bandpass filter (OBPF) to demultiplex the modulated signal. The OBPF was followed by an Rx-EDFA to provide constant power for optimized performance of the coherent receiver. The transmitted signals were then mixed with a 100 kHz linewidth local oscillator and the corresponding traces were captured with an 80 GSa/s, 36 GHz bandwidth real time oscilloscope. The detection procedure was followed by standard offline DSP for data recovery on the captured traces. The recorded symbols together

with the transmitted symbols were then used to derive the  $Q^2$  factor from the hard decision bit error rate (BER) [26,27]. The input and output optical spectrum after 20 span transmission can be seen in Fig. 4(a)–(d) where a maximum channel ripple (difference between the minimum and maximum channel peak powers) of 1.75 dB was observed for all our test cases.

## 5. Experimental results and discussions

To evaluate the impact of CD on a transmission link we compared the performance penalty in a fibre link with DCF and CRF in the DRA stages. These two fibres were chosen for a comparative study as their parameters are nearly identical apart from their value of CD which is  $-96$  ps/nm/km for DCF and  $11.7$  ps/nm/km for CRF (Table 1). Our experimental results in Figs. 5(a) and 5(b) show an enhanced performance of CRF (red circles) over DCF (blue diamonds) with a peak to peak (Pk-Pk)  $Q^2$  factor difference of  $\sim 0.8$  dB and  $\sim 1$  dB for  $20 \times 63$  km and  $30 \times 63$  km of transmission distance, respectively for a 10 channel WDM system. Also, the difference in the  $Q^2$  factor between CRF and DCF in the nonlinear regime of Fig. 5(a) and (b) increases with an increase in span number from 20 to 30, clearly indicating the accumulation of larger nonlinear noise in DCF in comparison to that of CRF. The experimental results in Fig. 5(a) and 5(b) suggest that the addition of dispersion in the DRA stages impacts the overall performance of the transmission system, and the penalty for this accumulated nonlinear noise is larger for negative CD fibre compared to positive CD fibre, implying that fibre with positive value of CD is a better choice for DRA-assisted coherent WDM systems.

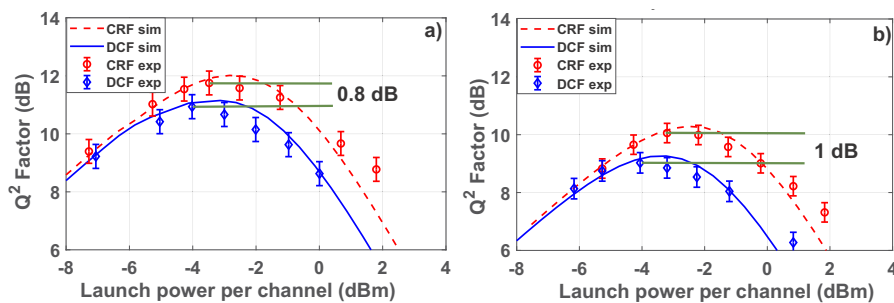


**Fig. 5.** a)  $Q^2$  factor vs launch power per channel, experimental and simulation results with CRF and DCF for a)  $20 \times 63$  km b)  $30 \times 63$  km transmission.

To further investigate the impact of nonlinear noise accumulation in a coherent WDM system with variation in nonlinear coefficient ( $\gamma$ ), we experimentally compared transmission performance with IDF ( $\gamma \sim 3.5 \text{ W}^{-1} \text{ km}^{-1}$ ) and CRF ( $\gamma \sim 8.9 \text{ W}^{-1} \text{ km}^{-1}$ ) in the DRA stage. This comparison is not ideal for our purposes because the CD of IDF and CRF are of opposite signs and the IDF loss is lower (Table 1), but nevertheless it is instructive. Our experimental results in Fig. 6(a) and 6(b) show a slightly enhanced performance of IDF (black squares) over CRF (red circles) for 20 and 30 span transmission with the Pk-Pk  $Q^2$  factor decreasing slightly from  $\sim 0.4$  dB to  $\sim 0.35$  dB. The enhanced performance of IDF over CRF can be attributed to its low attenuation coefficient, lower value of linear NF and lower nonlinear coefficient ( $\gamma$ ). However, an interesting observation to note here is that unlike our previous comparison between CRF and DCF in Fig. 5, the difference in the  $Q^2$  factor between IDF and CRF in the nonlinear regime of Figs. 6(a) and 6(b) actually decreases with increase in span number from 20 to 30. As above, this effect is due to the greater accumulation of nonlinear noise in IDF (previously DCF) in comparison to CRF, as a result of positive CD in CRF, but the effect is insufficient in this case to result in CRF outperforming IDF in terms of overall system performance. Nevertheless, our experimental results are sufficient to

suggest that a positive dispersion fibre with a value of nonlinear coefficient ( $\gamma$ ) similar to that of IDF would be a good choice of gain fibre for DRA-assisted transmission systems.

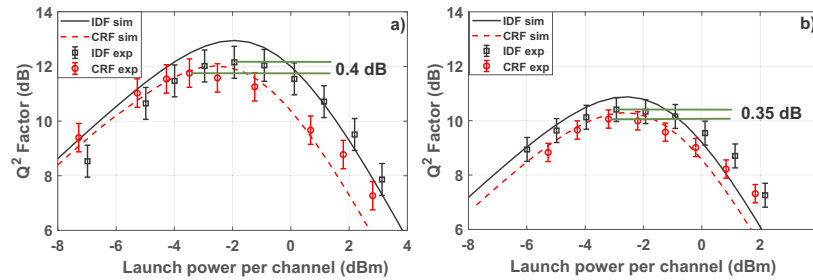


**Fig. 6.** a)  $Q^2$  factor vs launch power per channel, experimental and simulation results with CRF and IDF fibre for a)  $20 \times 63$  km b)  $30 \times 63$  km transmission.

The experimental results show a similar trend to the modelling predictions with a maximum difference of  $\sim 0.8$  dB between peak  $Q^2$  factors at optimum launch power for all test cases. Note, for the modelling, the additional linear ASE due to the loop EDFA was considered explicitly in the  $P_{ASE}$  term of Eq. (3), assuming a gain of 18dB and a fixed NF of 6dB. The fixed NF assumption may account for the experimental data in Figs. 5 and 6 showing relatively shallower reductions in  $Q^2$  factor with launch power.

We also measured the maximum reach at the optimum launch power with each DRA gain fibre (Fig. 7(a)). As expected, CRF and IDF outperformed DCF in terms of the peak  $Q^2$  factor with a maximum transmissible distance reaching out to  $\sim 2600$  km assuming a HD-FEC limit of 8.5 dB. By comparison, the maximum reach for DCF was limited to  $\sim 1900$  km. We attribute this enhanced performance of CRF over DCF to the high positive dispersion value @ 1550 nm, lowering the phase matching coefficient and resulting in a lower accumulated nonlinear noise. In the case of IDF, the enhanced performance over DCF and CRF can be attributed to its lower nonlinear coefficient leading to low nonlinear power accumulation and also its lower value of linear NF which improves the overall  $Q^2$  factor of the system.

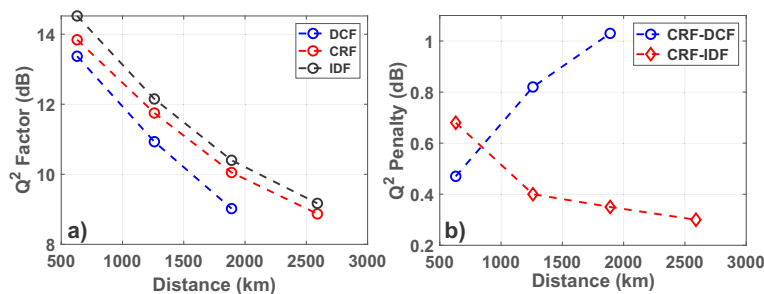


**Fig. 7.** 10 Channel 30 GBaud DP QPSK transmission a)  $Q^2$  Factor vs distance b)  $Q^2$  penalty (with respect to CRF-DCF and CRF-IDF) vs distance.

The  $Q^2$  penalty shown in Fig. 7(b) represents the experimental maximum Pk-Pk  $Q^2$  factor difference between two fibre types. For our first case, the  $Q^2$  penalty between CRF and DCF (dashed blue line with circles marker) has a positive slope with an increase in transmission distance, and the maximum  $Q^2$  penalty of  $\sim 1$  dB occurs at a transmission distance of  $\sim 1900$  km. The positive slope implies that positive CD fibre is preferable to negative CD fibre for a DRA transmission system, with the accumulated value of CD improving the overall performance.

In comparison, the  $Q^2$  penalty between CRF and IDF in Fig. 7(b) shows a negative slope (dashed red line with diamond markers). The  $Q^2$  penalty decreases from  $\sim 0.7$  dB at 600 km to  $\sim 0.3$  dB at 2600 km. This decrease in  $Q^2$  penalty shows that the accumulation of positive CD in CRF improves the overall transmission performance, but due to the lower nonlinear coefficient and lower linear NF of the IDF, CRF is unable to exceed its performance over IDF within the assumed range of HD-FEC limit of 8.5 dB. However, this advantage of IDF over CRF comes at a cost of higher pump power required for achieving a target gain.

## 6. Conclusions

In this paper, we evaluated the performance penalty due to discrete Raman amplifier in a coherent WDM system. To study the nature of the nonlinear product power addition in a coherent system with used three test fibres DCF, CRF and IDF as the gain fibre in the DRA stage of the transmission system. We used an analytical model with piecewise signal-profile approximation to calculate the nonlinear product power with varying CD and nonlinear coefficient. Our modelling results showed that a positive dispersion gain fibre with a nonlinear coefficient similar to that of IDF is a good choice for DRA assisted transmission system.

We further demonstrated experimentally the impact of CD and nonlinear coefficient using a recirculation loop transmission experiment. The long-haul transmission experiment was performed using 9 WDM ASE channels combined with a 30 GBaud DP-QPSK modulated signal at 1550 nm. Our experimental results with CRF and DCF in the DRA stage showed an enhanced performance of CRF over DCF in the nonlinear regime with a Pk-Pk  $Q^2$  factor difference of 0.8 and 1.0 dB for  $20 \times 63$  km and  $30 \times 63$  km of transmission distance. This enhanced performance can be attributed because of the accumulated residual dispersion due to positive CD in CRF. Our second set of test cases involved IDF and CRF as gain fibres in the DRA transmission system where a slightly improved performance of IDF over CRF was observed with the Pk-Pk  $Q^2$  factor difference decreasing from 0.4 dB to 0.35 dB for  $20 \times 63$  and  $30 \times 63$  km of transmission distance. The maximum transmission reach with IDF and CRF in the DRA stage was  $\sim 2600$  km, whereas for DCF it was  $\sim 1900$  km within a HD-FEC limit of 8.5 dB. Moreover, a positive slope for  $Q^2$  penalty was observed in the transmission performance between CRF and DCF, clearly indicating the improved performance of positive CD fibre versus negative CD fibre. In contrast, a negative slope for the  $Q^2$  penalty between CRF and IDF was observed, indicating that the slight performance improvement of IDF over CRF is due to its lower value of NF and lower nonlinear coefficient. Overall, our experimental and analytical modeling results clearly show that Raman gain fibre with positive chromatic dispersion is a better choice than its counterpart negative dispersion fibre, and with a nonlinear coefficient ( $\gamma$ ) of  $\sim 4W^{-1}km^{-1}$  similar to that of IDF, the corresponding fibre would be a good choice of Raman gain fibre for a DRA-based coherent WDM transmission system

**Funding.** H2020 Marie Skłodowska-Curie Actions (814276); Engineering and Physical Sciences Research Council (EP/V000969/1); Engineering and Physical Sciences Research Council (EP/M009092/1).

**Acknowledgement.** The authors thank Corning Incorporated for provision of the CRF and Lumentum UK for the loan of the transponder. The authors would also like to thank Dr Lukasz Krzczanowicz and Dr Pavel Skvortcov, now in Technical University of Denmark and Infinera Corporation for their technical support.

**Disclosures.** The authors declare no conflicts of interest.

**Data availability.** The original data for this work is available at Aston Research explorer [28].

## References

1. A. A. Al-Azzawi, A. A. Almukhtar, A. Dhar, M. C. Paul, H. Ahmad, A. Altuncu, R. Apsari, and S. W. Harun, "Gain-flattened hybrid EDFA operating in C + L band with parallel pumping distribution technique," *IET Optoelectron.* **14**(6), 447–451 (2020).
2. Y. Emori, K. Tanaka, and S. Namiki, "100 nm bandwidth flat-gain Raman amplifiers pumped and gain-equalised by 12-wavelength-channel WDM laser diode unit," *Electron. Lett.* **35**(16), 1355–1356 (1999).

3. M. N. Islam, "Raman amplifiers for telecommunications," *IEEE J. Sel. Top. Quantum Electron.* **8**(3), 548–559 (2002).
4. J. Bromage, "Raman Amplification for Fiber Communications Systems," *J. Lightwave Technol.* **22**(1), 79–93 (2004).
5. A. Ferrari, A. Napoli, J. K. Fischer, N. Costa, A. D'Amico, J. Pedro, W. Forsysiak, E. Pincemin, A. Lord, A. Stavdas, J. P. F. P. Gimenez, G. Roelkens, N. Calabretta, S. Abrate, B. Sommerkorn-Krombholz, and V. Curri, "Assessment on the Achievable Throughput of Multi-Band ITU-T G.652.D Fiber Transmission Systems," *J. Lightwave Technol.* **38**(16), 4279–4291 (2020).
6. L. Rapp and M. Eiselt, "Optical Amplifiers for Multi – Band Optical," *J. Lightwave Technol.* **40**(6), 1579–1589 (2022).
7. Y. Huang, J. Du, Y. Chen, K. Xu, and Z. He, "Machine Learning Assisted Inverse Design for Ultrafine, Dynamic and Arbitrary Gain Spectrum Shaping of Raman Amplification," *Photonics* **8**(7), 260 (2021).
8. S. Namiki and Y. Emori, "Ultrabroad-band Raman amplifiers pumped and gain-equalized by wavelength-division-multiplexed high-power laser diodes," *IEEE J. Sel. Top. Quantum Electron.* **7**(1), 3–16 (2001).
9. G. Rizzelli, M. A. Iqbal, F. Gallazzi, P. Rosa, M. Tan, P. Corredera, J. D. Ania-Castañón, and P. Harper, "FBG reflectivity impact on RIN in ultralong laser amplifiers," *Opt. Express* **24**(25), 29170 (2016).
10. M. Asif Iqbal, L. Krzczanowicz, I. Phillips, P. Harper, and W. Forsysiak, "150 nm SCL-band transmission through 70 km SMF using ultra-wideband dual-stage discrete raman amplifier," in *Optical Fiber Communications Conference and Exhibition (OFC)* (2020), (c), pp. 1–3.
11. S. Liang, S. Jain, L. Xu, K. R. H. Bottrill, N. Taengnoi, M. Guasoni, P. Zhang, M. Xiao, Q. Kang, Y. Jung, P. Petropoulos, and D. J. Richardson, "High Gain, Low Noise, Spectral-Gain-Controlled," *J. Lightwave Technol.* **39**(5), 1458–1463 (2021).
12. C. Headley and G. P. Agrawal, "Raman Amplification in Fiber Optical Communication Systems," in *Chapter 5* (Elsevier Academic Press, 2005), pp. 217–234.
13. P. Hazarika, M. Abu-romoh, M. Tan, L. Krzczanowicz, T. T. Nguyen, M. A. Iqbal, I. Phillips, P. Harper, Ming-Jun Li, and W. Forsysiak, "Impact of Chromatic Dispersion in Discrete Raman Amplifiers on Coherent Transmission Systems," in *2021 Optical Fiber Communications Conference and Exhibition (OFC)* (OSA, 2021), pp. 1–3.
14. P. Poggiolini, A. Carena, V. Curri, G. Bosco, and F. Forghieri, "Analytical modeling of nonlinear propagation in uncompensated optical transmission links," *IEEE Photonics Technol. Lett.* **23**(11), 742–744 (2011).
15. A. Carena, V. Curri, G. Bosco, P. Poggiolini, and F. Forghieri, "Modeling of the impact of nonlinear propagation effects in uncompensated optical coherent transmission links," *J. Lightwave Technol.* **30**(10), 1524–1539 (2012).
16. M. J. Li, S. Li, and D. A. Nolan, "Nonlinear fibers for signal processing using optical Kerr effects," *J. Lightwave Technol.* **23**(11), 3606–3614 (2005).
17. L. Krzczanowicz, M. A. Z. Al-Khateeb, M. Asif Iqbal, and I. Phillips, P. Harper and W. Forsysiak, "Performance estimation of discrete Raman amplification within broadband optical networks," in *Optical Fiber Communication Conference (OFC) 2019* (OSA, 2019), pp. 1–3.
18. M. A. Z. Al-Khateeb, M. Tan, M. A. Iqbal, M. McCarthy, P. Harper, and A. D. Ellis, "Four wave mixing in distributed Raman amplified optical transmission systems," in *2016 IEEE Photonics Conference, IPC 2016* (2017), pp. 795–796.
19. M. A. Z. Al-Khateeb, M. A. Iqbal, M. Tan, A. A. I. Ali, M. McCarthy, P. Harper, and A. D. Ellis, "Analysis of the nonlinear Kerr effects in optical transmission systems that deploy optical phase conjugation," *Opt. Express* **26**(3), 88–93 (2018).
20. K. O. Hill, D. C. Johnson, and B. S. Kawasaki, "cw three-wave mixing in single-mode optical fibers," *J. Phys.* **49**(10), 5098–5106 (1978).
21. M. A. Iqbal, M. A. Z. Al-Khateeb, L. Krzczanowicz, I. D. Phillips, P. Harper, and W. Forsysiak, "Linear and Nonlinear Noise Characterisation of Dual Stage Broadband Discrete Raman Amplifiers," *J. Lightwave Technol.* **37**(14), 3679–3688 (2019).
22. N. Shibata, R. P. Braun, and R. G. Waarts, "Phase-Mismatch Dependence of Efficiency of Wave Generation Through Four-Wave Mixing in a Single-Mode Optical Fiber," *IEEE J. Quantum Electron.* **23**(7), 1205–1210 (1987).
23. M. Eiselt, "Impact of non-linear fiber effects on fiber choice for ultimate transmission capacity," in *Conference on Optical Fiber Communication Technical Digest Series* (2000), 1, pp. 58–60.
24. K. Inoue, "Phase-mismatching characteristic of four-wave mixing in fiber lines with multistage optical amplifiers K," *Opt. Lett.* **17**(11), 801–803 (1992).
25. C. Kurtzke, "Suppression of Fiber Nonlinearities by Appropriate Dispersion Management," *IEEE Photonics Technol. Lett.* **5**(10), 1250–1253 (1993).
26. A. D. Ellis, M. E. McCarthy, M. A. Z. Al Khateeb, M. Sorokina, and N. J. Doran, "Performance limits in optical communications due to fiber nonlinearity," *Adv. Opt. Photonics* **9**(3), 429 (2017).
27. I. D. Phillips, M. Tan, M. F. C. Stephens, M. E. McCarthy, E. Giacomidis, S. Sygletos, P. Rosa, S. Fabbri, S. T. Le, T. Kanesan, S. K. Turitsyn, N. J. Doran, P. Harper, and A. D. Ellis, "Exceeding the nonlinear-shannon limit using raman laser based amplification and optical phase conjugation," in *Optical Fiber Communication Conference, OFC 2014* (2014), pp. 5–7.
28. P. Hazarika, M. Tan, M. A. Iqbal, I. Phillips, P. Harper, J. Stone S, M. J. Li, and W. Forsysiak, "Performance Evaluation of Discrete Raman Amplifiers in Coherent Transmission Systems," Aston University (2022). <https://doi.org/10.17036/researchdata.aston.ac.uk.00000580>